

MOLDING THE FLOW OF LIGHT

A new class of materials, called photonic crystals, affects a photon's properties in much the same way that a semiconductor affects an electron's properties. The ability to mold and guide light leads naturally to novel applications in several fields, including optoelectronics and telecommunications. The authors present an introductory survey of the basic concepts and ideas, including results for never before possible photon phenomena.

For the past 50 years, semiconductor physics has played a vital role in almost every aspect of modern technology. Advances in this field have let scientists tailor the conducting properties of certain materials and initiate the transistor revolution in electronics. New research suggests that we might now be able to tailor the properties of light. The key in achieving this goal lies in the use of a new class of materials called *photonic crystals*,¹ whose underlying concept stems from Eli Yablonovitch's² and Sajeev John's pioneering work.³ The basic idea is to design materials that can affect photon properties in much the same way that ordinary semiconductor crystals affect electron properties. You achieve this control by constructing a crystal consisting of a periodic array of macroscopic uniform dielectric (or possibly metallic) "atoms." In this crystal, we can describe photons in terms of a band structure, as in the case of electrons.

Of particular interest is a photonic crystal whose band structure possesses a complete photonic *band gap*, a range of frequencies for which

light is forbidden to propagate inside the crystal. Light is forbidden unless there is a defect in the otherwise perfect crystal. A defect can lead to localized photonic states in the gap, whose shapes and properties would be dictated by the defect's nature. Moreover, a significant and attractive difference between photonic crystals and electronic semiconductor crystals is the former's inherent ability to provide complete tunability. A defect in a photonic crystal could, in principle, be designed to be of any size, shape, or form and could be chosen to have any of a wide variety of dielectric constants. Thus, defect states in the gap could be tuned to any frequency and spatial extent of design interest. In addition to tuning the frequency, we also control the localized photonic state's symmetry.

All these capabilities provide a new dimension in our ability to mold or control the properties of light. In this sense, defects are good. And herein lies the exciting potential of photonic crystals. Photonic crystals let us manipulate light in ways never before possible. This article's purpose is to highlight some of these novel possibilities. Here, computation plays a particularly important role. Indeed, unlike electronic structure in semiconductors, photonic crystals are unique in that a computer can calculate phenomena described by Maxwell's equations to any desired degree of accuracy. Thus, computer calculations and de-

1521-9615/01/\$10.00 © 2001 IEEE

STEVEN G. JOHNSON, ATTILA MEKIS, SHANHUI FAN, AND
JOHN D. JOANNOPOULOS
Massachusetts Institute of Technology

sign play particularly important and complementary roles in experimental investigations of photonic crystals.

Computational methods

We can cast Maxwell's equations for the propagation of light in mixed, loss-less dielectric media in a form reminiscent of Schrödinger's equation. Consequently, we can use techniques for studying electrons in solids to study photon modes in photonic crystals.^{4,5} The main differences are that electrons are described by a complex *scalar* field and strongly interact with each other, whereas photons are described by a *vector* field and do not interact with each other. For all practical purposes, then, solution of photon equations leads to an exact description of their properties, which represents one of the few cases in science where computer experiments can be almost as accurate as laboratory experiments.

There are two types of numerical methods that we employ to study photonic crystals: *time domain*, a numerical experiment in which we simulate the time evolution of Maxwell's equations directly, and *frequency domain*, in which we solve for time-harmonic eigenmodes (band structures, for example, or dispersion relations) of light in a structure. To solve Maxwell's equations in 3D for periodic dielectric media in the time domain, we employ Yee-lattice finite difference time domain (FDTD) methods, which can include periodic as well as absorbing boundary conditions.⁶

To solve Maxwell's equations in 3D for periodic dielectric media in the frequency domain, we begin by expanding the fields in plane-waves. As in the case of electrons, the use of a plane-wave basis set has several desirable consequences.⁵ First, the set is complete and orthonormal. Second, finite sets can be systematically improved straightforwardly. Third, a priori knowledge of field distribution is not required to generate the set. Fourth, the constraint of divergentless fields is easily maintained. Finally, there are extremely reliable and efficient methods for calculating eigenfields, such as preconditioned conjugate gradients.

The chief difficulty in using plane waves appears to be that huge numbers of plane waves are required to describe the rapid changes in the dielectric constant of photonic crystals. But this is not the case because we can easily overcome the potential problem with a better treatment of the boundaries between dielectric media. In partic-

ular, construction of a dielectric tensor to interpolate in the boundaries can lead to a rapid convergence of all eigenmodes,⁴ improving by over an order of magnitude on previous techniques. Thus, a combination of this interpolation scheme together with a conjugate gradient approach can lead to an efficient method for frequency domain calculations.

A simple model system

In this article, we introduce concepts and properties that are generally valid in 3D photonic crystals, but for the sake of simplicity, our examples involve 2D photonic crystals. We begin by considering a perfect array of infinitely long dielectric rods located on a square lattice of lattice constant a , and we investigate the propagation of light in the plane that is normal to the rods. The rods have a radius of $0.20a$ and a refractive index of 3.4, which corresponds to GaAs at a wavelength of 1.55 microns.

Such a structure possesses a complete gap between the first and second transverse magnetic modes. For TM modes, the electric field is parallel to the rods. Once we have a band gap, we can introduce a defect inside the crystal to trap or localize light. In particular, we outline defects and defect complexes that correspond to specific components and devices such as wave guides, wave guide bends, microcavities, and channel-drop filters.

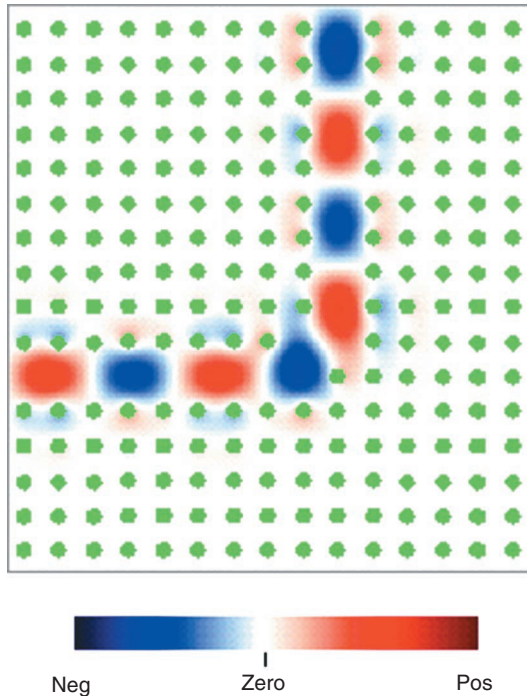
Photonic crystal wave guides

By making a line defect, we can create an extended mode that we can use to guide light. Traditionally, you achieve wave guiding in dielectric structures, such as optical fibers, by total internal reflection. When the fibers are bent very tightly, however, the angle of incidence becomes too large for total internal reflection to occur, and light escapes at the bend. Photonic crystals can be designed to confine light even around tight corners because they do not rely on the angle of incidence for confinement.

To illustrate this point, we remove a row of dielectric rods from the photonic crystal described earlier. This introduces a single guided-mode band inside the gap. The field associated with the guided mode is strongly confined in the vicinity of the defect and decays exponentially in

Defects are good. And herein lies the exciting potential of photonic crystals.

Figure 1. An electric field pattern in the vicinity of a sharp 90-degree bend. The electric field is polarized along the axis of the dielectric rods. The green circles indicate rod position. Unlike the mechanism of total internal reflection, a photonic crystal allows light to be guided in air.



the crystal. An intriguing aspect of photonic crystal wave guides is that they provide a unique way to guide optical light, tractably and efficiently, through narrow channels of air. Once light is introduced inside the wave guide, it has nowhere else to go. The only source of loss is reflection from the wave guide input, which suggests that we might use photonic crystals to guide light around tight corners, as in Figure 1.

Although the bend's radius of curvature is less than the light's wavelength, nearly all the light is transmitted through the bend over a wide range of frequencies through the gap. The small fraction of light that is not transmitted is reflected. For specific frequencies, we can achieve 100 percent transmission.⁷ Note that a critical and necessary condition for 100 percent transmission efficiency is that the photonic crystal wave guide be single-mode in the frequency range of interest.

Figure 2 illustrates a recent experimental verification of 100 percent transmission efficiency at sharp bends. These are results from Shawn-Yu Lin and others⁸ who performed experiments at microwave length scales for a series of wave guide bends (similar to the configuration in Figure 1) using an appropriately scaled square lattice of alumina rods in air. The red circles are experimental measurements, and the blue circles are theoretical prediction, illustrating good agreement over a wide range of frequencies.

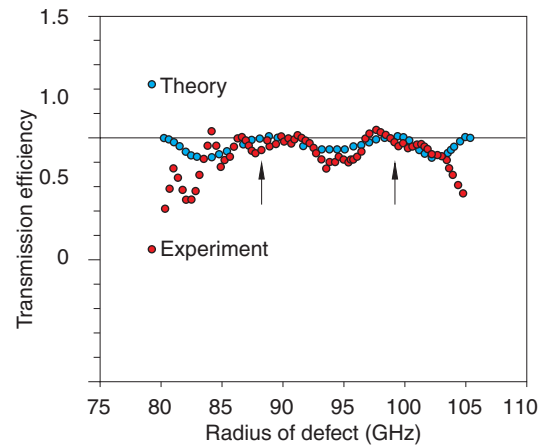


Figure 2. Transmission efficiency around a sharp 90-degree bend for a wave guide carved out of a square lattice of alumina rods in air. The red circles represent experimental measurements, and the blue circles represent theoretical prediction.

Photonic crystal microcavities

In addition to making line defects, we can also create local imperfections that trap light at a point within the crystal. As a simple example, we can choose a single rod and form a defect by changing its radius. Figure 3 shows the defect-state frequencies for several values of the defect radius. We begin with the perfect crystal—where every rod has a radius of $0.20a$ —and gradually reduce a single rod's radius.

As the radius of the defect rod is reduced, a singly degenerate symmetric localized state appears in the defect's vicinity. Because the defect involves removing dielectric material in the crystal, the state appears at a frequency close to the band gap's lower edge. As the rod's radius is further reduced, the defect state's frequency sweeps upward across the gap.

Instead of reducing a rod's size, we could make it larger. Starting again with a perfect crystal, we gradually increase the rod's radius. When the radius reaches $0.25a$, two doubly degenerate modes appear at the top of the gap. Because the defect involves adding material, the modes sweep downward across the gap as we increase the radius. They eventually disappear into the continuum (below the gap) when the radius becomes larger than $0.40a$. The electric fields of these modes have two nodes in the plane and are thus dipolar in symmetry. If we keep increasing the radius, a large number of localized modes can be created in the defect's vicinity.

Several modes appear at the top of the gap:

first a quadrupole, then another nondegenerate quadrupole, followed by a second-order monopole and two doubly degenerate hexapoles. We can tune the resonant mode's frequency and symmetry simply by adjusting the rod's size. One important aspect of a finite-sized microcavity is its quality factor Q , roughly $\lambda/\delta\lambda$ where $\delta\lambda$ is the width of the cavity resonance, a dimensionless measure of the resonant state's lifetime.

Pete Villeneuve and others⁹ have studied a finite-sized crystal made of dielectric rods where a single rod has been removed. They verified that the value of Q increases exponentially with the number of surrounding rods and found that it reaches a value close to 10^4 with as little as four rods on either side of the defect. Note also that these cavities possess small modal volumes, on the order of $(\lambda/2n)^3$. The combination of large quality factor with small modal volume offers a unique capability of maximally enhancing spontaneous emission.

Channel-drop filters

One of the most prominent devices in the telecommunications industry is the channel-drop filter. This prominence is a consequence of both its importance and its size (roughly 10×10 cm). Channel-dropping filters are necessary for manipulating wavelength-division multiplexed optical communications, where one channel is dropped at one carrier wavelength, leaving all other channels unaffected. Photonic crystals pre-

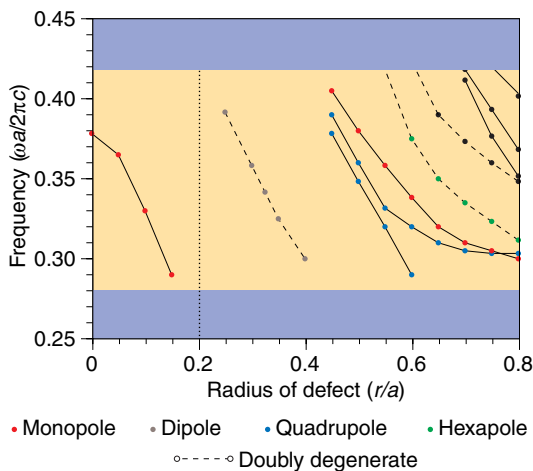


Figure 3. Defect states introduced in the gap by changing a single rod's radius in an otherwise perfect square lattice of dielectric rods in air. When the radius is $0.2a$, there is no defect; when the radius is 0, the rod is completely removed. The shaded regions indicate the band gap's edges.

sent a unique opportunity to investigate the possibilities of miniaturizing devices to the scale of the wavelength of interest, 1.55 microns.

We combined line defects and point defects to make a novel photonic crystal channel-drop filter that gives access to one channel of a wavelength-division multiplexed signal while leaving other channels undisturbed. We created two parallel wave guides—a main transmission line and a secondary wave guide—inside a photonic crystal by removing two rows of dielectric rods. We introduced a resonant cavity between the two wave guides by creating one or more local defects. Resonant cavities are attractive candidates for channel dropping because we can use them to select a single channel with a very narrow line width.

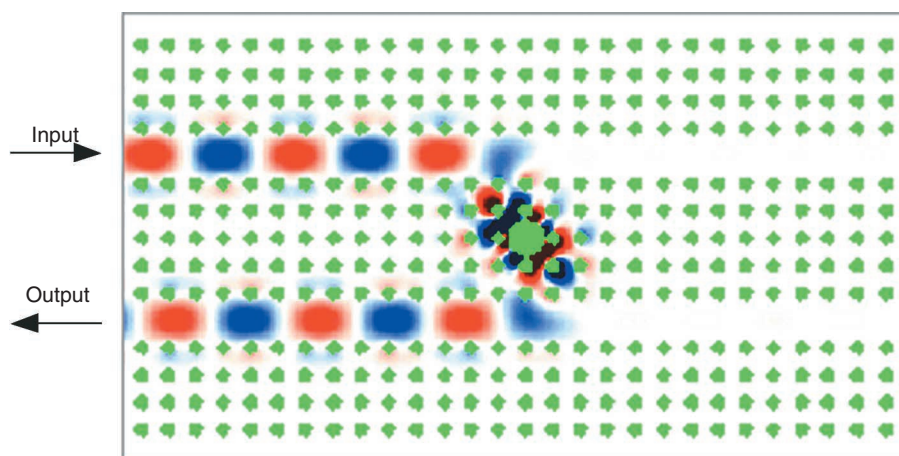
The filter performance is determined by the transfer efficiency between the two wave guides. Perfect efficiency corresponds to complete transfer of the selected channel—in either the forward or backward direction in the secondary wave guide—with no forward transmission or backward reflection in the main transmission line. All other channels remain unaffected by the optical resonator's presence. Shanhui Fan and others^{10–11} have proved that the coupling resonator must satisfy three conditions to achieve optimal channel-dropping performance:

1. The resonator must possess at least two resonant modes, each of which must be even and odd, respectively, with regard to the mirror plane of symmetry perpendicular to the wave guides.
2. The modes must be degenerate (or nearly so). The system's intrinsic symmetry does not support degeneracies, so you must force an accidental degeneracy.
3. The modes must have equal Q (or nearly so).

All three conditions are necessary to achieve complete transfer. The reflected amplitude in the transmission line originates solely from the decay of the localized states. The reflection therefore will not be canceled if the optical resonator supports only a single mode. To ensure the reflected signal's cancellation, the structure must possess a plane of mirror symmetry perpendicular to both wave guides, and must support two localized states with different symmetry with respect to the mirror plane, one even and one odd.

Because the states have different symmetries, tunneling through each one constitutes an inde-

Figure 4. Steady-state field distribution of the photonic crystal channel-drop filter at resonance. This device's size is on the order of the light's wavelength in air.



pendent process. The even state decays with the same phase along both the forward and backward directions while the odd state decays with opposite phase. When the two tunneling processes are combined—because of the phase difference—the decaying amplitudes cancel along the backward direction of the transmission line. For cancellation to occur, the line shapes of the two resonances must overlap. Because each resonance possesses a Lorentzian line shape, both resonances must have the same center frequency and the same width. When such degeneracy occurs, the incoming wave interferes destructively with the decaying amplitude along the forward direction in the transmission line, leaving all the power to be transferred into the secondary wave guide at the resonant frequency.

A photonic crystal system provides precisely the control necessary to satisfy all three conditions. Figure 4 shows an example of a photonic crystal channel-drop filter. The cavity consists of a single point defect with a radius of $0.60a$. As we already saw in Figure 3, this defect supports a doubly degenerate hexapole state near $\omega_0 = 0.39$ ($2\pi c/a$) with the required symmetry. However, the presence of the wave guides next to the cavity breaks the degeneracy of the hexapoles. To restore the degeneracy, we change the dielectric constant (or the size) of two rods adjacent to the defect. By properly changing the rods, we can affect the modes in different ways and force an accidental degeneracy in frequency.

An approximate degeneracy in width exists between the states because the hexapoles possess large enough orbital angular momentum to ensure roughly equal decay of the even and odd modes in the wave guides. We simulate the structure's filter response by sending a pulse through the upper wave guide. The transmission

in the main line is close to 100 percent for every channel, except at the resonant frequency, where the transmission drops to 0 percent and the transfer efficiency approaches 100 percent. The quality factor is larger than 6,000. Because the even state (with respect to the mirror plane perpendicular to the wave guides) is odd with respect to the mirror plane parallel to the wave guides, the transfer occurs along the backward direction in the secondary wave guide. Finally, although the line shape of the current resonant modes is Lorentzian, we can modify it to the preferred square wave shape by introducing complexes of coupled resonant modes.¹²

Photonic crystal slabs

Photonic crystal slabs have attracted much interest^{13–25} because of their relative ease of fabrication at micron-length scales compared to 3D photonic crystal structures. They are a hybrid system combining photonic crystal guiding in the plane and conventional index guiding (total internal reflection) vertically. Because they do not exhibit a complete photonic band gap, it is impossible to prevent radiation losses (vertical scattering) whenever translational symmetry is entirely broken—for example, by a resonant cavity or a wave guide bend.

In some cases, you might want radiation,¹⁶ but for planar optical devices, vertical scattering will generally be a loss mechanism that you want to minimize.

The radiation Q_{\perp}

As discussed earlier, a resonant cavity of Lorentzian line shape is described by a quality factor, Q , which we can also define as the number of cycles for its energy to decay by $e^{-2\pi}$. The

decay rate $1/Q$ is thus the bandwidth at half maximum of any filter or other device based on the cavity. A typical cavity has several decay mechanisms, each of which is described by its own lifetime. First, there are the radiation losses, characterized by Q_{\perp} (perpendicular to the slab)—which is the same as the total Q in an infinite, perfect crystal. Then, there are in-plane losses, Q_{\parallel} , due to the crystal's finite size. These losses decrease exponentially as the crystal size increases. There are also losses due to absorption and disorder, which we do not consider in this article. Finally, there is the rate at which the light decays where you want it to go—in an adjacent wave guide for a filter, for example, described by some Q_d (device). The total Q is then²⁶

$$Q = [Q_d^{-1} + Q_{\perp}^{-1} + Q_{\parallel}^{-1}]^{-1}. \quad (1)$$

Because we can make Q_{\parallel} effectively infinite, Q_{\perp} determines an upper bound on the achievable total Q of the device. Moreover, the fraction of energy lost to radiation is given by^{22,26}

$$\left(\frac{Q}{Q_{\perp}}\right)^2 = \left(\frac{Q_d}{Q_{\perp} + Q_d}\right)^2. \quad (2)$$

So, as long as Q_{\perp} is much larger than Q_d , the radiation losses will be small. As a corollary, if Q_d is small, then Q_{\perp} need not be high to achieve low losses. Because light decays quickly in a wave guide from a bend, small Q_{\perp} can be tolerated there. Large Q_{\perp} , however, is required for the case of high Q devices or cavities we consider here. Thus, our goal is to maximize Q_{\perp} .

The model slab system

The model system that we consider is a square lattice of finite-height dielectric rods in air (with lattice constant a , radius $0.2a$, height $2a$, and a dielectric constant ϵ of 12, which corresponds to Si at 1.55 microns). This structure is depicted along with its band diagram in Figure 5. The computation (using the frequency domain method) and analysis of this band structure is described elsewhere²⁵ and exhibits several important features.

The shaded region—the light cone—is the projection of all possible modes propagating in the air above and below the slab. The bands below the light cone cannot couple to it and are guided. They are extended in the plane but decay exponentially above and below it and never scatter perfectly. These guided bands are divided according to whether they are even or odd with respect to the horizontal mirror plane bisecting the slab. In

this article, we concentrate on the modes of odd symmetry, which possess a band gap—a range of frequencies in which no guided modes exist—and are strongly analogous to the TM modes in the corresponding 2D system. In the mirror plane itself, the even and odd modes are purely TE/TM polarized. The slab's height is critical to achieve a large band gap and to prevent higher-order modes from impinging on the gap.

To analyze resonant cavities formed by point defects in the crystal, we used FDTD calculations with absorbing boundary conditions. The computational cell was an 11×11 lattice of rods, with the defects at the center surrounded by a margin of $4a$ above and below the rods and $2a$ on the sides. Around the sides of the crystal, we included a dielectric slab the same height as the rods and extending to the cell's boundaries, separated from the edge of the crystal by $0.5a$. This slab's purpose is to leech off whispering-gallery modes associated with the entire crystal, which otherwise have long lifetimes. It does not appreciably affect the radiation Q_{\perp} of the cavities and only affects the in-plane Q_{\parallel} .

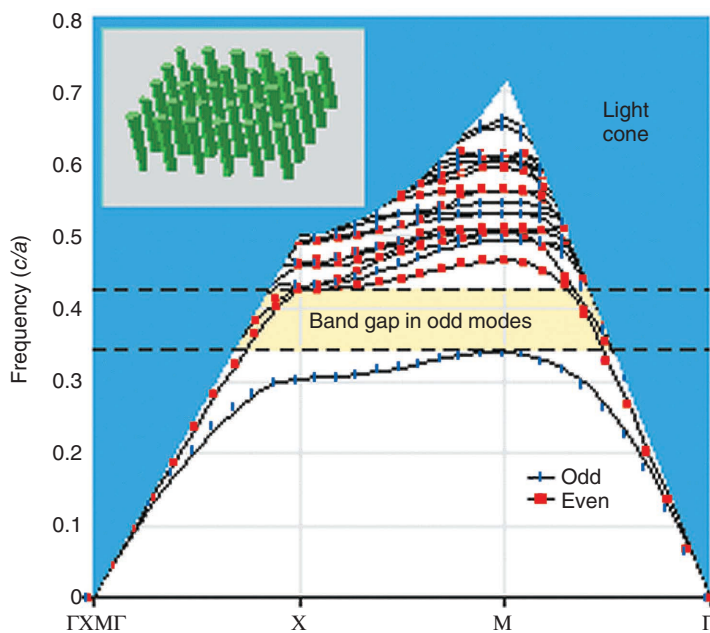


Figure 5. A projected band diagram for a square lattice (lattice constant a) of dielectric cylinders (radius $0.2a$, height $2a$, $\epsilon = 12$) in air, computed in 3D and plotted for Bloch wave vectors on the boundary of the 2D irreducible Brillouin zone. The bands below the shaded region (the light cone) are vertically guided within the slab and do not scatter. These guided bands are either even (red squares) or odd (blue ticks) with respect to the mirror symmetry plane bisecting the slab.

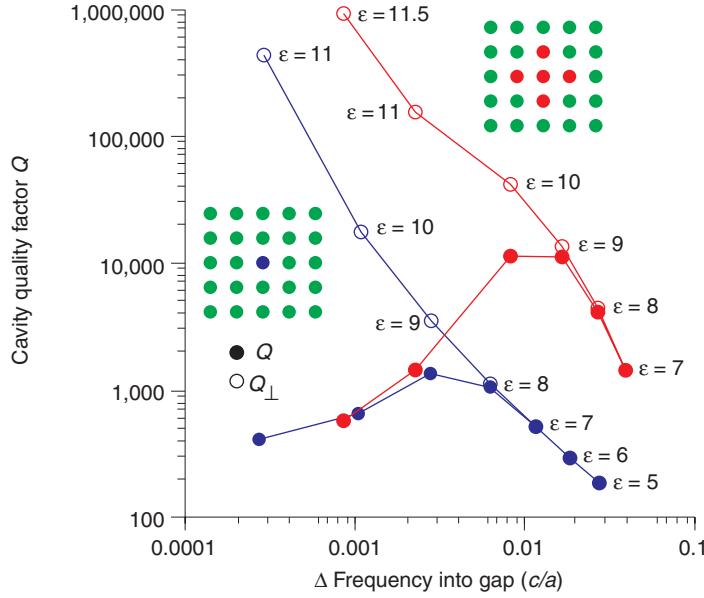


Figure 6. Total Q (solid circles) and radiation Q_{\perp} (hollow circles) plotted versus $\Delta\omega$ above the band edge for monopole defects in an 11×11 slab of rods from Figure 5. Blue points are for a single-rod defect and red points are for a five-rod super-defect.

The FDTD grid resolution is 10 pixels per a . At this resolution, the cylinders are blocky but are nevertheless periodic, and the basic photonic band gap and guiding phenomena are not altered. We also tried some cases at 15 pixels per a and obtained consistent results. There is a frequency shift, however, relative to the higher-resolution calculations in Figure 5, so we recomputed the odd-mode band gap using a single-rod FDTD calculation with Bloch-periodic boundary conditions at the sides (analyzing the spectrum excited by point sources as below), and found it to lie from 0.320 to 0.391 c/a .

We excite the cavity's defect modes with one or more dipole sources arranged in the same symmetry as the mode of interest. From the field amplitude as a function of time at a point in the cavity, we extract the mode frequencies and decay constants by the filter diagonalization method using a Fourier basis.²⁷ To determine Q_{\perp} and Q_{\parallel} , we run the simulation again with Gaussian sources narrowly peaked around the desired mode's frequency. With only this mode excited, we measure the vertical flux through planes above and below the rods and the horizontal flux through planes at the cell's edges (extending to a height $0.5a$ above and below the rods). The lifetimes in each direction are then given by²⁸

$$Q_{\perp,\parallel} = \frac{\omega U}{P_{\perp,\parallel}}. \quad (3)$$

Here, ω is the angular frequency, U is the total electromagnetic energy, and P is the radiated power; U and P are time-averaged. We verified the results to be consistent with Equation 1.

Mode delocalization

Spatial delocalization of a cavity mode generally leads to increased Q_{\perp} . Because the mode becomes more delocalized as it approaches the band gap's edges (the unperturbed states), we expect that Q_{\perp} will not peak at mid-gap but might increase toward one or both band edges.

You can see the relationship between Q_{\perp} and localization in several ways. The more spatially delocalized the mode is, the more localized it will be in wave vector space. That is, a definite wave vector and translational symmetry are approximately regained, and we can prevent coupling to the light cone by momentum conservation just as in the bulk slab or in linear wave guides. We can make a more rigorous argument in the Green's function formalism, in which the radiated field can be obtained from the field at the defect:

$$\vec{E}(\vec{r}) = \int \hat{G}_{\omega}(\vec{r}, \vec{r}') \Delta\epsilon(\vec{r}') \omega^2 \vec{E}(\vec{r}') d^3\vec{r}'. \quad (4)$$

Here, \hat{G}_{ω} is the Green's function operator of the unperturbed crystal, $\Delta\epsilon$ is the defect's change in the dielectric function, and ω is the mode frequency. This equation suggests two ways to decrease the radiated field: Either delocalize the mode to decrease the field at the defect or reduce the perturbation $\Delta\epsilon$ (which delocalizes the field, too).

To illustrate this effect, we create a monopole-like point defect in the photonic crystal slab by changing a single rod's ϵ . Figure 6 shows the resulting Q as a function of ω . As expected, Q_{\perp} diverges toward the lower band edge (the source of the defect mode), while Q_{\parallel} peaks toward mid-gap (where the field is most localized and does not see the crystal edges), with the total Q dominated by the smallest of the two.

Another way to delocalize the mode, achieving greater delocalization for the same frequency, is to enlarge the defect's size. In this case, we change ϵ in a five-rod super-defect. The results, also shown in Figure 6, display the same general behavior as a single defect but with dra-

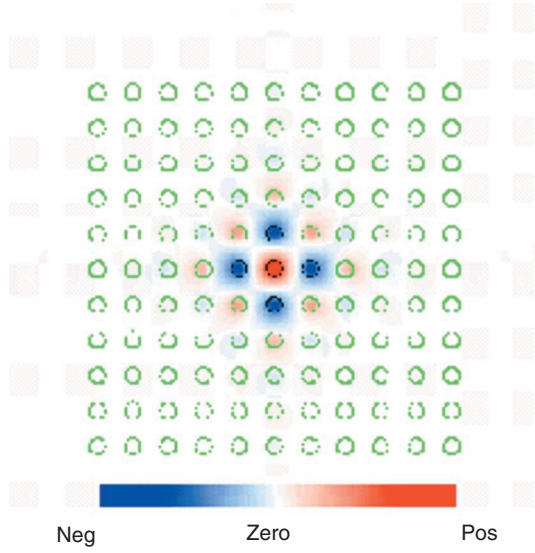


Figure 7. Monopole defect mode for $\epsilon = 9$ super-defect ($Q = 11,000$, $Q_{\perp} = 13,000$): electric field z-component in the plane bisecting the rods.

matically increased Q . A total Q of over 10^4 is obtained for a defect ϵ of 9, five percent above the gap bottom, testifying to the localization of the state in Figure 7.

To completely understand the super-defect, we must consider coherent scattering. In effect, the super-defect forms a tiny photonic crystal slab whose guided modes only scatter from the boundaries. As the number of rods in the super-defect is increased, it will eventually become multimode, but in this case the cavity is single-mode.

A disadvantage of the delocalization method is that it increases the modal volume V . For example, increasing the modal volume could reduce the enhancement factor η of spontaneous emission in a cavity, which goes like Q/V . We can estimate Q and η from the last equation by assuming that \hat{G}_{ω} and \vec{E} are approximately constant inside the defect and neglecting coherence, in which case we find with the help of Equation 3 that

$$Q_{\perp} \sim \frac{\langle |\vec{E}|^2 \rangle}{\Delta\epsilon^2 \langle |\vec{E}|^2 \rangle_{\text{defect}}} \sim \frac{V}{\Delta\epsilon^2} \sim \frac{1}{\Delta\epsilon^2 \Delta\omega^{d/2}}. \quad (5)$$

Here, $\Delta\omega$ is the frequency above the gap edge and d is the number of dimensions we are delocalizing. The decay length is proportional to $\Delta\omega^{-1/2}$. It follows that η is proportional to $\Delta\epsilon^{-2}$ and thus the increase in Q outpaces the increase in V for small perturbations.

We can apply this inverse relationship between localization and Q to other systems. Other research addresses a 2D analog²⁹ and applies it to cavities in a photonic crystal slab of holes rather than rods.²² Alternatively, the state can be delocalized vertically using a low-contrast slab and operating above the light line. In this case, we can make a similar argument using the Green's function of the 2D photonic crystal.³⁰ The relevant band edge there is that of the mode propagating vertically along the 2D defect, which might lie in the 2D band gap's interior since horizontal localization is not sacrificed. In such conventional structures as ring resonators, Q again grows with increasing size in a phenomenon conceptually similar to that of the super-defect.

In principle, the same effect could occur at both band edges, but several things can prevent it from being observable, especially at the upper band edge. For example, there can be a finite threshold required in $\Delta\epsilon$ before a mode is localized. Or the upper boundary of the gap can be other than the perturbed mode's band edge.

Far-field cancellation

There is also a conceptually different mechanism for minimizing a cavity's radiation losses, one that does not require state delocalization and that can peak anywhere in the gap's interior rather than only at a band edge.²⁹ If the field oscillates in sign, especially for a higher-order mode in which the differing signs have equal magnitude, it might be possible to force cancellations in the far-field radiation pattern (of Equation 4) by varying $\Delta\epsilon$. You would thus be left with higher-order multipole far-field radiation components, which are expected to radiate less power than the lowest-order multipole far-field component of a highly localized source.

We can illustrate this effect in the photonic crystal slab of rods by first creating a near-field quadrupole point-like defect by increasing the radius of a rod to $0.45a$ and increasing its ϵ to 13. To achieve the far-field quadrupole-component cancellation, we need an extra tuning parameter for $\Delta\epsilon$, which can be achieved by increasing the radii of the four adjacent rods to $0.25a$ and varying their dielectric constants to adjust the mode frequency. In principle, we can vary radii alone, but this is limited in our case by the finite computational resolution. Figure 8 shows the results of this exercise.

Note that Q and Q_{\perp} are essentially the same due to the in-plane localization. Q peaks at 1,925

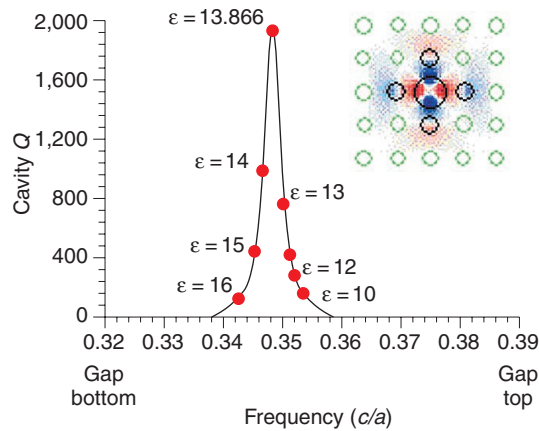


Figure 8. Total Q plotted versus frequency for a quadrupole state where the frequency range is the gap. The state is formed by defect of an $r = 0.45a$ central rod with $\epsilon = 13$, and four $r = 0.25a$ neighbor rods whose ϵ was varied to control ω . The solid line is a Lorentzian curve fitted to the peak (with $R^2 = 0.9994$).

in the gap's interior, so the underlying phenomenon must differ from the delocalization mechanism discussed previously. To verify that the peak is due to the postulated far-field cancellation, in Figure 9 we plot the fields for ω below, at, and above the peak. In Figure 9a, the TM electric field at midplane shows that all the near-field patterns remain quadrupole and are almost identical, independent of the far-field multipole symmetry. However, Figure 9b shows that the radiated energy density $2a$ above the rods exhibits two clear nodal planes that are introduced precisely at the peak, as expected. The introduction of these nodal planes reveals a cancellation of the lowest-order far-field quadrupole component, leaving only higher-order far-field multipole components that radiate less power. In con-

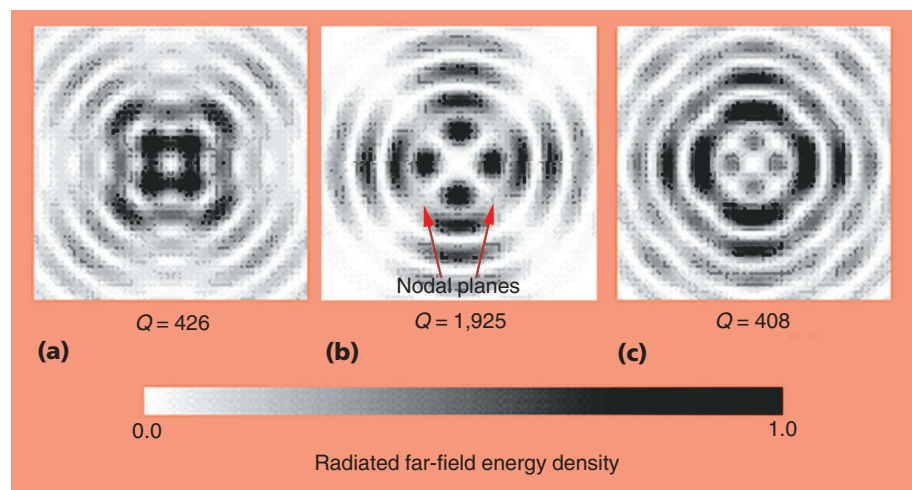
trast, if the dielectric constants or radii of all five defect rods are increased together, Q increases monotonically toward the lower band edge just as in Figure 6 without far-field nodal planes.


This particular cavity is a proof of concept. We expect that significant refinements (increased Q , for example) are possible. A similar peaking of Q in the gap's interior (with a peak value of more than 10^4) was reported in a photonic crystal slab of holes, and we suspect that the explanation is that there must also be a far-field cancellation.²⁸

Presently in telecommunications and optoelectronics there is a great drive toward miniaturizing optical devices to the point where we are approaching the scale of the wavelength itself. The goal is eventually to integrate such devices onto a single chip. To achieve such localization, however, it might be necessary to exploit mechanisms that go beyond index guidance (total internal reflection). Photonic crystals provide a new and promising foundation on which to build future optical systems.

A key problem in the design of future integrated optical devices is how to balance ease of fabrication with the reduction of radiation losses. Photonic crystal structures with 3D periodicity provide the ultimate in radiation control but currently pose substantial fabrication challenges. Consequently, 2D periodic photonic crystal structures, which are much easier to fabricate, are an attractive alternative if they can be designed to achieve acceptable losses. In addition to the intrinsic radi-

Figure 9. Far-field patterns for Figure 8's quadrupole mode, for points (a) just before ($Q = 426$, $\omega = 0.346$), (b) at ($Q = 1,925$, $\omega = 0.349$), and (c) just beyond ($Q = 408$, $\omega = 0.352$) the peak. The electric field energy density is plotted in a plane $2a$ above the rods. Note the appearance of nodal planes at the peak. In contrast, the near-field pattern (as shown in Figure 8) is indistinguishable for all these points.



ation losses of any localized optical component in a slab structure, an important concern for future research is the characterization and control of losses due to fabrication-related disorder. 

Acknowledgments

This work is supported in part by the MRSEC program of the NSF under award DMR-9400334. We also acknowledge the valuable contributions of our collaborator Pete Villeneuve.

References

- J.D. Joannopoulos, R.D. Meade, and J.N. Winn, *Photonic Crystals*, Princeton Univ. Press, New York, 1995.
- E. Yablonovitch, "Inhibited Spontaneous Emission in Solid-State Physics and Electronics," *Physical Rev. Letters*, vol. 58, no. 2509, 1987.
- S. John, "Strong Localization of Photons in Certain Disordered Dielectric Superlattices," *Physical Rev. Letters*, vol. 58, 1987, pp. 2486–2489.
- R.D. Meade et al., "Accurate Theoretical Analysis of Photonic Band-Gap Materials," *Phys. Rev. B*, vol. 48, no. 11, 1993, pp. 8434–8437.
- S.G. Johnson and J.D. Joannopoulos, "Block-Iterative Frequency-Domain Methods for Maxwell's Equations in a Planewave Basis," *Optics Express*, vol. 8, no. 173, 2001, pp. 173–190.
- K.S. Yee, *IEEE Trans. Ant. Prop.*, vol. 14, no. 302, 1966.
- A. Mekis et al., "High Transmission through Sharp Bends in Photonic Crystal Waveguides," *Physical Rev. Letters*, vol. 77, 1996, pp. 3787–3790.
- S.Y. Lin, *Science*, vol. 282, no. 274, 1998.
- P.R. Villeneuve, S. Fan, and J. D. Joannopoulos, "Microcavities in Photonic Crystals: Mode Symmetry, Tunability, and Coupling Efficiency," *Phys. Rev. B*, vol. 54, 1996, pp. 7837–7842.
- S. Fan et al., "Channel Drop Tunneling through Localized States," *Physical Rev. Letters*, vol. 80, 1998, pp. 960.
- S. Fan et al., "Channel Drop Filters in Photonic Crystals," *Optics Express*, vol. 3, no. 4, 1998, pp. 4–11.
- S. Fan et al., "Theoretical Analysis of Channel Drop Tunneling Processes," *Phys. Rev.*, vol. 59, 1999, pp. 15882–15892.
- R.D. Meade et al., "Novel Applications of Photonic Band Gap Materials: Low-Loss Bends and High-Q Cavities," *J. Applied Physics*, vol. 75, 1994, pp. 4753–4755.
- P.L. Gourley et al., "Optical Properties of Two-Dimensional Photonic Lattices Fabricated as Honeycomb Nanostructures in Compound Semiconductors," *Applied Physics Lett.*, vol. 64, 1994, pp. 687.
- T. Kraus, R. De La Rue, and S. Band, "Two-Dimensional Photonic-Bandgap Structures Operating at Near-Infrared Wavelengths," *Nature*, vol. 383, 1996, pp. 699.
- S. Fan et al., "High Extraction Efficiency of Spontaneous Emission from Slabs of Photonic Crystals," *Physical Rev. Letters*, vol. 78, no. 3294, 1997, pp. 3294.
- B. D'Urso et al., "Modal Reflectivity in Finite-Depth Two-Dimensional photonic crystal Microcavities," *J. Opt. Soc. Am.*, vol. 15, Mar. 1998, pp. 1155–1159.
- M. Kanskar et al., "Observation of Leaky Modes in an Air-Bridged Semiconductor Waveguide with a Two-Dimensional Photonic Lattice," *Applied Physics Lett.*, vol. 70, 1997, p. 1438.
- M.D.B. Charlton, S.W. Roberts, and G.J. Parker, "Guided Mode Analysis and Fabrication of a 2-Dimensional Visible Photonic Band Structure Confined within a Planar Semiconductor Waveguide," *Materials Science and Eng.*, vol. B49, no. 155, 1997.
- Y. Chen et al., "Fabrication of Two-Dimensional Photonic Lattices in GaAs: The Regular Graphite Structures," *Superlattices and Microstructures*, vol. 22, no. 109, 1997.
- D. Labilloy et al., "Quantitative Measurement of Transmission, Reflection, and Diffraction of Two-Dimensional Photonic Band Gap Structures at Near-Infrared Wavelengths," *Physical Rev. Letters*, vol. 79, 1997, p. 4147.
- P.R. Villeneuve et al., "Three-Dimensional Photon Confinement in Photonic Crystals of Low-Dimensional Periodicity," *IEEE Proc. Optoelec.*, vol. 145, 1998, p. 384.
- R. Coccioli, "What is the Smallest Possible Electromagnetic Mode Volume in a Dielectric Cavity?" *IEEE Proc. Optoelec.*, vol. 145, no. 391, 1998.
- M. Boroditsky, R. Coccioli, and E. Yablonovitch, *Proc. SPIE*, vol. 3283, no. 1, 1998.
- S.G. Johnson et al., "Guided Modes in Photonic Crystal Slabs," *Physical Rev.*, vol. 60, 1999, pp. 5751–5758.
- H.A. Haus, *Waves and Fields in Optoelectronics*, Prentice-Hall, Englewood Cliffs, N.J., 1984.
- V.A. Mandelstam and H. S. Taylor, "Harmonic Inversion of Time Signals and Its Applications," *J. Chem. Phys.*, vol. 107, 1997.
- O.J. Painter et al., "Defect Modes of a Two-Dimensional Photonic Crystal in an Optically Thin Dielectric Slab," *J. Opt. Soc. Am.*, vol. 16, no. 275, Feb. 1999, pp. 275–285.
- J.D. Joannopoulos et al., "Novelties of Light with Photonic Crystals," *Proc. NATO ASI 2000: Photonic Crystals and Light Localization*, to be published.
- H. Benisty et al., "Radiation Losses of Waveguide-Based Two-Dimensional Photonic Crystals: Positive Role of the Substrate," *Applied Physics Letters*, vol. 76, Jan. 2000, pp. 532–534.

For more information on this or any other computing topic, please visit our Digital Library at <http://computer.org/publications/dlib>.

Steven G. Johnson is a postdoctoral fellow at MIT. His research interests include photonic crystals, optical physics, and novel computational algorithms. He received a PhD from MIT. Contact him at stevenj@alum.mit.edu.

Attila Mekis is a staff scientist at Clarendon Photonics. His research interests include integrated optical systems for opto-electronics and telecommunications. He received a PhD from MIT. Contact him at mekis@clarendonphotonics.com.

Shanhui Fan is an assistant professor at Stanford University. His research interests include photonic crystals, quantum optics, and optical physics. He received a PhD from MIT. Contact him at shanhui@stanford.edu.

John D. Joannopoulos is the Francis Wright Davis Professor of Physics at MIT. His research interests include photonic crystals and condensed matter physics. He received a PhD from Berkeley. Contact him at joannop@mit.edu.